Available online at www.sciencedirect.com
ScienceDirect
Physics Letters B 649 (2007) 35–42
PHYSICS LETTERS B
www.elsevier.com/locate/physletb

Experimental determination of the J^π components of the spin-dipole resonance in ^{12}B

M.A. de Huu [a,1], A.M. van den Berg [a], N. Blasi [b], R. De Leo [c], M. Hagemann [d,2], M.N. Harakeh [a], J. Heyse [d,3], M. Hunyadi [a,4], S. Micheletti [b], H. Okamura [e], H.J. Wörtche [a,*]

[a] *Kernfysisch Versneller Instituut, University of Groningen, NL-9747 AA Groningen, The Netherlands*
[b] *Istituto Nationale di Fisica Nucleare, Sezione di Milano, Via Celoria 16, 20133 Milano, Italy*
[c] *Istituto Nationale di Fisica Nucleare, Sezione di Bari, Via Orabona 4, 70126 Bari, Italy*
[d] *Vakgroep Subatomaire en Stralingsfysica, Universiteit Gent, Proeftuinstraat 86, B-9000 Gent, Belgium*
[e] *Research Center for Nuclear Physics, Osaka University, Ibaraki, Osaka 567-0047, Japan*

Received 18 October 2006; received in revised form 4 February 2007; accepted 5 March 2007

Available online 23 March 2007

Editor: V. Metag

Abstract

The inclusive ^{12}C($\vec{d}$, ^{2}He) and exclusive ^{12}C($\vec{d}$, ^{2}He + n) reactions have been studied with a beam energy of 171 MeV and scattering angles for the (d, ^{2}He) reaction $\theta = 0°$ and 3°. The studies focused on the separation of the isovector spin-dipole resonance (IVSGDR) into its components by measuring tensor-analysing powers and observing the direct neutron decay to the low-lying proton-hole states in ^{11}B. Merging the information obtained from both measurements resulted in the first-time verification of model-independent predictions of tensor-analysing powers at extreme forward angles and the experimental decomposition of the IVSGDR into its J^π components. The experimental results are in reasonable agreement with theoretical estimates based on shell-model calculations.

PACS: 26.50.+x; 25.45.Kk; 27.40.+z; 25.45.-z

In the past years, many experiments have been dedicated to the investigation of Gamow–Teller (GT) transitions in atomic nuclei. The characteristics of a GT transition is given by a change of the nuclear spin S and the nuclear isospin I by one unit, i.e. $\Delta S = \Delta I = 1$, and no orbital angular momentum transfer, $\Delta L = 0$. Because of the simple structure of the transition operator, experimental GT strength distributions provide excellent testing grounds for nuclear-structure model predictions. Moreover, GT strength distributions are correlated to intriguing issues of astrophysics and fundamental physics. In the calculation of weak-interaction rates of processes taking place during the last phase of a heavy star in its presupernova stage GT transitions in fp-shell nuclei play a decisive role [1,2]. Most commonly, the experimental investigations take advantage of charge-exchange reactions at intermediate energies because they naturally induce isovector transitions. By varying the bombarding energy, selectivity in the excitation of spin-flip transitions can be achieved, owing to the different energy dependence of the various terms in the nucleon–nucleon interaction [3].

In comparison to GT transitions, experimental studies of the higher multipole spin–isospin excitations are more involved because the associated transitions are shifted to higher excitation energies and the strength distributions are more spread. In the present work we focus on the experimental investigation of the $\Delta S = \Delta L = 1$ spin-dipole resonance (IVSGDR), the so-called first forbidden GT strength. Due to the finite orbital angular

* Corresponding author.
E-mail address: h.j.woertche@kvi.nl (H.J. Wörtche).
[1] Present address: Contrinex SA, route André Piller 50, 1762 Givisiez, Switzerland.
[2] Robert Bosch GmbH, D-71229 Leonberg, Germany.
[3] Present address: SCK·CEN, Boeretang 200, 2400 Mol, Belgium.
[4] Present address: Institute of Nuclear Research of the Hungarian Academy of Sciences, 4001 Debrecen, Hungary.

0370-2693/$ – see front matter
doi:10.1016/j.physletb.2007.03.031

momentum transfer the IVSGDR splits into three components having $J^\pi = 0^-, 1^-, 2^-$ when the target nucleus has $J^\pi = 0^+$. Besides the location of IVSGDR, the identification of the J^π components has gained special attention. This is not the least due to the requirements imposed by the theoretical interpretation of $0\nu2\beta$-decay measurements where the J^π components of the IVSGDR provide significant contributions to the nuclear transition-matrix element and experimental information on the decomposition of the IVSGDR provides important calibration for theory (see e.g. [4]). A special challenge is posed by the identification of the $J^\pi = 0^-$ component, which is the most elusive component and which is not accessible to electromagnetic probes. The collective $J^\pi = 0^-$ component of the IVSGDR is considered to act as mediator for parity mixing in complex nuclear states and the excitation energy is sensitive to the treatment of pion exchange in the nuclear potential [5].

To study the J^π components of higher multipole spin–isospin excitations, especially the $\Delta S = \Delta L = 1$ IVSGDR, an even more selective probe compared to standard charge-exchange reactions is required to identify the states of interest. The $(\mathrm{d}, {}^2\mathrm{He})$ reaction at intermediate energies is a very clean filter to study spin–isospin excitations [6]. The two protons in the ejectile are referred to as ^{2}He to indicate that the two protons are coupled to an unbound $^1S_0$ state. If one uses a purely tensor-polarised deuteron beam, the $(\vec{\mathrm{d}}, {}^2\mathrm{He})$ reaction can be thought of, from a naïve point of view, as an $(\vec{\mathrm{n}}, \vec{\mathrm{p}})$ reaction with spin-flip where the proton in the projectile acts as a spectator. The $(\vec{\mathrm{d}}, {}^2\mathrm{He})$ reaction would then yield the same information as the $(\vec{\mathrm{n}}, \vec{\mathrm{p}})$ reaction [7], but under experimentally more favourable conditions. This method has first been developed at Laboratoire National Saturne at beam energies ranging from 0.6 to 2.0 GeV [8] and has since then been applied at RIKEN at a bombarding energy of 270 MeV [9,10] and in the course of this work, for the first time at KVI, with an unprecedented energy resolution of 130 keV FWHM at $E_d = 170$ MeV.

Most commonly, the polarisation observables in a nuclear reaction are described in the right-handed Cartesian coordinates of the helicity frame, where the z-axis coincides with the incoming beam direction, the y-axis is defined by the normal to the scattering plane and the x-axis by its orthogonality to the y- and z-axes to complete a right-handed coordinate system. Usually the polarisation state of a particle beam is defined with respect to an axis of symmetry defined by the magnetic field of the ion source. If this is chosen to be the Z-axis of a right-handed coordinate system, the Y-axis can be chosen to be orthogonal to this Z-axis and the beam direction, and finally the X-axis is chosen to complete a right-handed coordinate system of the source frame. In this coordinate system, the polarisation of the deuteron-beam particles can be represented by an incoherent mixture of N_+ particles with the spin aligned along the Z-direction ($m = +1$), N_- particles with spin along the Z-direction ($m = -1$) and N_0 particles with spins uniformly distributed in the X, Y-plane ($m = 0$). Within this framework, the vector polarisation p_Z and the tensor polarisation p_{ZZ} are defined by

$$p_Z = N_+ - N_- \quad \text{and} \quad p_{ZZ} = N_+ + N_- - 2N_0, \tag{1}$$

respectively, with the normalisation $N_+ + N_- + N_0 = 1$. In case of a purely tensor-polarised beam ($p_Z = 0$), p_{ZZ} can take values ranging between -2 and 1, the lower limit corresponding to $N_0 = 1$ and the upper one to $N_+ = N_- = \frac{1}{2}$.

The $(\mathrm{d}, {}^2\mathrm{He})$ cross-section for a purely tensor-polarised deuteron beam is given in case the polarisation is orthogonal to the beam direction by [11]

$$\frac{d\sigma(\theta,\varphi)}{d\Omega} = \left(\frac{d\sigma(\theta)}{d\Omega}\right)_0 \Big[1 - \frac{1}{4} p_{ZZ} A_{zz}(\theta) - \frac{1}{4} p_{ZZ}\big(A_{zz}(\theta) + 2A_{yy}(\theta)\big)\cos 2\varphi\Big], \tag{2}$$

with $(\frac{d\sigma}{d\Omega})_0$ is the unpolarised cross section and θ and φ are the polar and azimuthal scattering angles. In Eq. (2), the polarisation parameters p_Z and p_{ZZ} are defined in the source frame and the Cartesian tensor analysing powers A_{ii} in the helicity frame. At $\theta = 0^\circ$ (180°) for target nuclei with ground-state spin $J^\pi_{\mathrm{g.s.}} = 0^+$, for which the spin-parity structure of the reaction is $1^+ + 0^+ \to 0^+ + J^\pi$, the model-independent relations $A_{zz} = -2$ for a $J^\pi = 0^-$ state and $A_{zz}(0^\circ) = 1$ and $A_{xx}(0^\circ) = A_{yy}(0^\circ) = -\frac{1}{2}$ for natural-parity states hold at 0° [10,12]. From these relations a straightforward identification of two of the three IVSGDR components should be possible. At finite scattering angles the A_{yy} dependence vanishes from the cross section formula Eq. (2) if the ^{2}He detector has a 2π coverage in the azimuthal scattering angle φ. In this case one can directly extract A_{zz}. If the coverage of the azimuthal scattering angle φ is small, $\cos(2\varphi)$ in Eq. (2) can be approximated by 1 and one can extract A_{yy}. This goes, however, at a dramatic cost of acceptance at forward angles. In the present experiment, a purely tensor-polarised deuteron beam provided by the polarised ion source POLIS [13] was accelerated to 171 MeV by the superconducting cyclotron AGOR. The beam impinged on natural carbon targets of 9.4 mg/cm^2 (flexible graphite, 99.8%) and 23 mg/cm^2 (rigid graphite, 99.95%), respectively. The beam polarisation changed in intervals of 5 minutes between the unpolarised state and two purely tensor-polarised states with average values of $p_{ZZ} = -1.24$ and $p_{ZZ} = 0.57$. The correlated proton pairs stemming from the $(\mathrm{d}, {}^2\mathrm{He})$ charge-exchange reaction were detected with the Big-Bite magnetic Spectrograph (BBS) [14] in conjunction with the EuroSuperNova detection system [15]. The BBS was set at central scattering angles $\theta_{\mathrm{BBS}} = 0^\circ$ and 3°. The beam line to the spectrometer was set up for dispersion-matched transport to achieve optimum energy resolution. Neutrons emitted at backward angles with respect to the beam direction (110°–160°) were detected in 32 liquid-scintillator detectors from the EDEN detection system [16]. The neutron energies were determined by time-of-flight (TOF) measurements using digital techniques to separate events induced by neutrons and γ's in the EDEN system. A special scattering chamber with a thin wall of 2 mm stainless steel was used to reduce re-scattering of neutrons. Typical beam current values were 0.1 to 0.5 nA, again depending on the target thickness. The primary trigger rate was around 20–30 kHz in the ESN detector system, yielding a two-proton coincidence rate of 2 Hz and a (triple) neutron coincidence rate of 0.02–0.06 Hz, depending

on the target thickness. All measurements were performed with a dead-time of 25 to 30%.

The choice of ^{12}C as a target was based on two considerations: First, ^{12}C has been often investigated using various (d, ^{2}He) [9,10,17], (n, p) [18–20] and (p, n)-type experiments [17,20–26], and second, ^{12}C is a light nucleus, for which background considerations are not yet critical, and serves, therefore, as a benchmark to study the eventual application of this method to heavier nuclei.

The objective of the experiment was two-fold. First objective was the first-time experimental verification of the model-independent predicted analysing powers quoted above. In this context, we took advantage of the unique energy resolution achieved for (d, ^{2}He) at KVI which provided the opportunity to extract analysing powers for the well-resolved low-lying excited states in ^{12}B. The (d, ^{2}He) data set was analysed using the procedure described in [6]. The second goal was to locate the IVSGDR in ^{12}B and to decompose it into its components. A problem one faces when experimentally studying giant resonances is the combination of two effects: their widths and the underlying continuum background. To get a handle on the latter, coincidences between the ejectile ^{2}He at forward angles and decay neutrons emitted at backward angles with respect to the beam direction were required, which significantly reduced continuum background mainly due to knock-on charge-exchange process.

The description of the non-resonant continuum background present in charge-exchange reactions is usually done in a phenomenological way first described by Erell et al. [27]. The main contribution of the continuum can be ascribed to quasi-free scattering, where the reaction is assumed to proceed through a collision with a single nucleon, for which the kinematics are closely related to the free-scattering process. The shape of the background can be approximated by [27]

$$\frac{d^2\sigma}{d\Omega\, dE} = N\,\frac{1-\exp[-(E_x-E_0)/T]}{1+[(E_x-E_{\mathrm{QF}})/W_L]^2}, \quad E_x > E_0, \tag{3}$$

where E_0 is the neutron separation energy in ^{12}B (3.37 MeV), E_{QF} is given by the kinematics of the actual reaction on a proton target (-12.53 MeV at $\theta_{\mathrm{lab}} = 1^\circ$), N is a scattering-angle-dependent normalisation factor, W_L is the width of the quasi-free peak and T is a cut-off-energy parameter. The three variables N, W_L and T are adjustable parameters. In the present analysis, the values $W_L = 7.5$ MeV and $T = 4.0$ MeV were taken from an analysis performed by Okamura et al. [10] of ^{12}C(d, ^{2}He)^{12}B data measured at $E_d = 270$ MeV. The value of T was adjusted to 4.5 MeV for a better agreement with the data at lower excitation energy and the amplitude N was fitted to match the data. The resulting approximation of the continuum background is shown in the top-left panel of Fig. 1. The validity of the background approximation by a quasi-free continuum has been checked by comparing with the cross sections measured in coincidence with decay neutrons detected at backward angles. The spectra in the lower panels of Fig. 1 show the striking similarity between the singles spectrum after subtraction of the quasi-free continuum (QFC) presented in the upper-right panel of Fig. 1 and the coincidence data. This similarity strongly suggests the validity of the background approximation. It is interesting to note, that for both spectra no structure is observed above $E_x = 14$ MeV in ^{12}B, indicating that quasi-free scattering is the dominating contribution in this range.

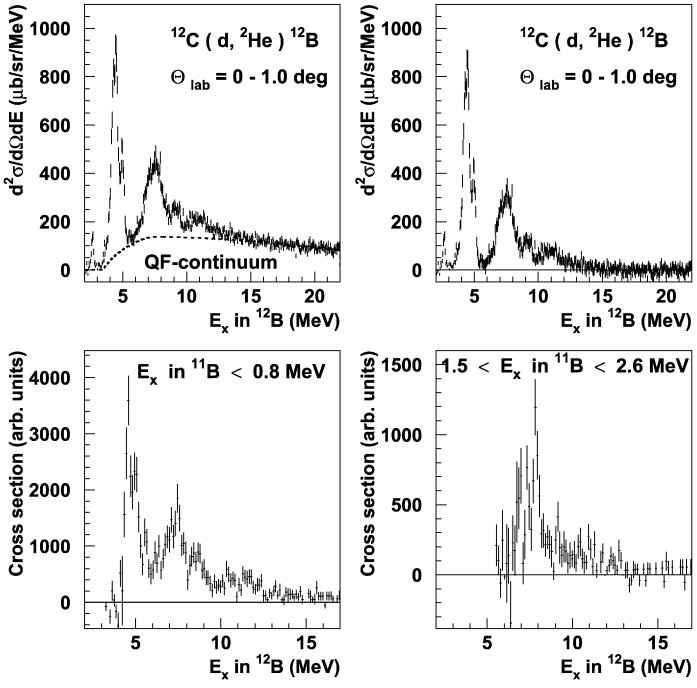

Fig. 1. Upper panels: singles spectrum of the ^{12}C(d, ^{2}He)^{12}B reaction with an estimate of the quasi-free continuum (QFC) (left panel) and spectrum after the QFC subtraction (right panel). Lower panels: coincidence spectra for which a coincidence with a neutron populating the ground state (left panel) and the first-excited state (right panel) in ^{11}B is required.

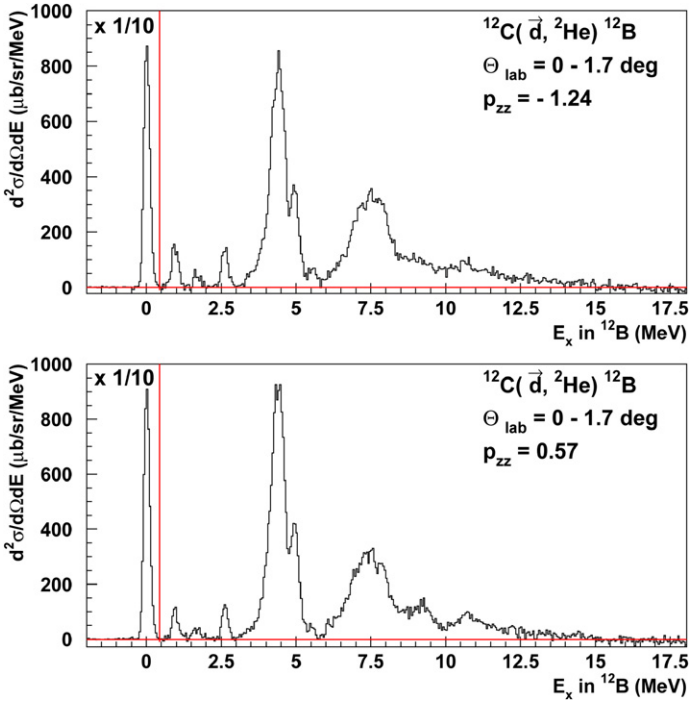

Fig. 2. Double-differential cross sections for the ^{12}C($\vec{d}$, ^{2}He)^{12}B reaction in the angular bin $\theta_{lab} = 0°$–$1.7°$ for the different tensor-polarisation states of the beam.

Singles spectra for the two beam tensor polarisations are shown in Fig. 2 after subtraction of QFC. Besides the ground-state transition, which has been downscaled for reasons of representation, several low-lying, well-resolved transitions can clearly be identified. The structure around $E_x = 4.4$ MeV is considered to contain most of the 2^- component of the IVS-GDR, the peak at $E_x = 5.0$ MeV is a known GT transition [28]. Additional weak transitions can be detected around $E_x = 5.5$ and 6.1 MeV. A broad structure in the cross section around $E_x = 7.5$ MeV, for which no definite conclusions about its spin and parity exist, is also strongly excited.

To extract angular distributions of cross sections and analysing powers, the excitation-energy spectra between $E_x = 3.0$–5.4 MeV were fitted using the code FIT [29]. Owing to too many unknowns in the level scheme, no consistent fit could be performed beyond $E_x = 5.2$ MeV and the analysis was done per bins of 50 and 100 keV.

Due to the very small residual background, cross sections have been extracted for all states up to $E_x = 3$ MeV by placing markers and summing up the counts. The decomposition of the structure between $E_x = 3.0$–5.4 MeV was performed by fitting it with four Voigt functions, as shown in Fig. 3. The instrumental width parameter was determined by fitting the peak for the ground-state transition with a Voigt function with a Lorentz width $\Gamma = 0$ keV which yielded a FWHM of 130 keV for the thin target and FWHM of 225 keV for the thicker target, respectively. In the combined analysis, the energy spectra measured with the thin target were folded with a Gaussian to adjust the energy resolution. This decomposition was the only one providing a consistent description of the data for the different scattering-angle bins. The small peak at $E_x = 3.75$ MeV, tabulated in Ref. [28], was introduced to improve the quality of the fit. However, because of the systematic uncertainties, no cross sections are presented. The structure around $E_x = 4.4$ MeV was decomposed into two peaks centred around $E_x = 4.21(1)$ MeV and $E_x = 4.47(1)$ MeV, with widths $\Gamma = 260$ keV and $\Gamma = 209$ keV, respectively. The level at $E_x = 4.21$ MeV does not match the entries in Ref. [28]. To eliminate any ambiguity, these two peaks have been analysed as one, i.e. their areas have been added. The peak around $E_x = 5$ MeV (the fitted value of the centroid is 4.95(1) MeV, with a width $\Gamma = 60$ keV) is a known $J^\pi = 1^+$ level [28]. The widths were kept identical for each scattering-angle bin.

The DWBA cross-section and analysing-power calculations for the different transitions have been performed using the code ACCBA of Okamura [30], which is specialised for the (d, ^{2}He) reaction. The optical-model parameters and further input parameters were taken from literature [31]. In all calculations, the D-wave contribution of the incident deuteron and the outgoing ^{2}He was not taken into account, because its effect is exceedingly small at the forward angles of interest [30].

The measured and calculated cross sections and tensor-analysing powers for well-resolved states up to $E_x = 5$ MeV are compared in Fig. 4 for positive-parity transitions and Fig. 5 for negative-parity transitions. The corresponding values for the most forward ^{2}He detection angle are listed in Table 1. For the first time, predictions for the tensor-analysing powers A_{yy} and A_{zz} based on symmetry arguments for natural-parity states using the (d, ^{2}He) reaction could be compared with experimental data. This was not possible in Ref. [10] because of lack of statistics. From Figs. 4 and 5 one can deduce, that for the natural-parity states at $E_x = 0.96$ and $E_x = 2.62$ MeV the tensor-analysing powers A_{zz} and A_{yy} nicely match the predictions, i.e. $A_{zz} = 1$ and $A_{yy} = -0.5$ at $\theta = 0°$. This indicates

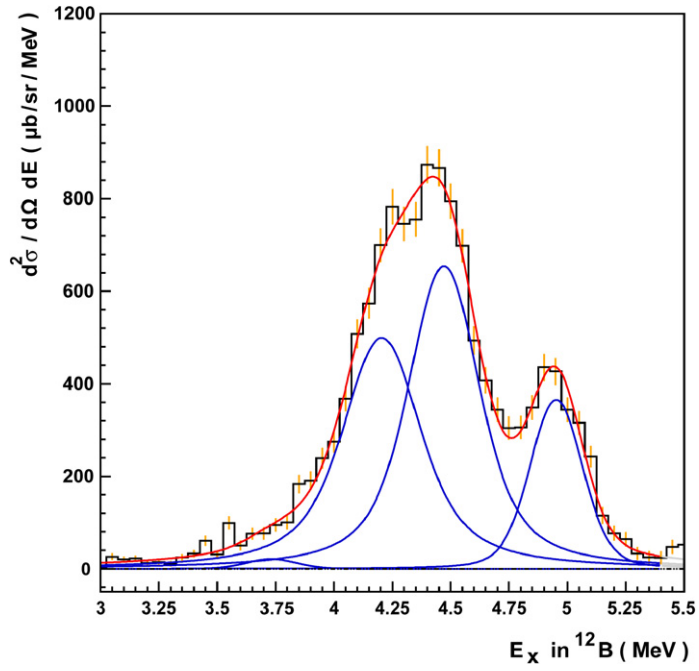

Fig. 3. Decomposition of the bumps around $E_x = 3.0$–5.4 MeV into four Voigt functions in the angular bin $\theta_{\text{lab}} = 0°$–$1.7°$.

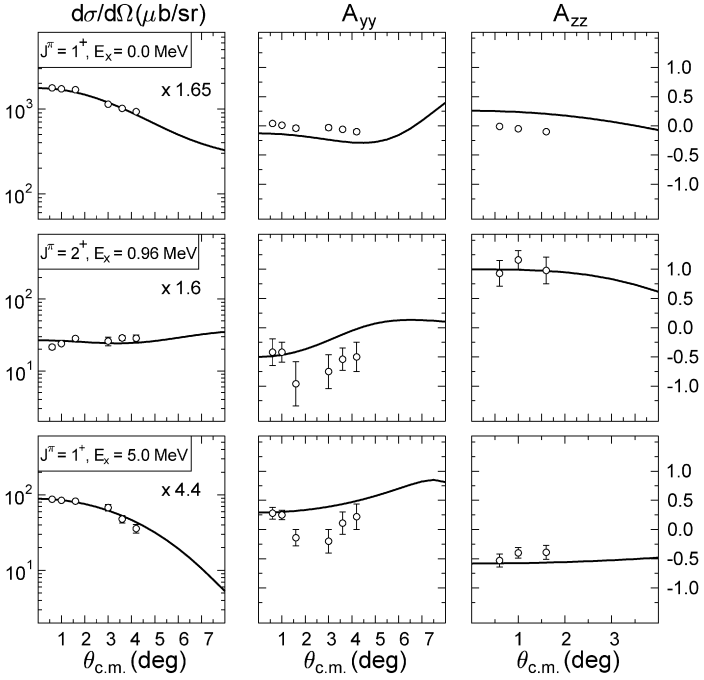

Fig. 4. Measured and calculated $^{12}\text{C}(\vec{\text{d}}, ^2\text{He})^{12}\text{B}$ differential cross sections and tensor-analysing powers for some positive-parity low-lying excited states. The scaling factors of the DWBA cross sections are indicated.

that the analysing powers of tensor polarised (d, ^{2}He) provides a sensitive tool to identify natural-parity states at extreme forward scattering angles.

The difference between the double-differential cross sections for the two beam polarisations for the angular bin $\theta_{\text{lab}} = 0°$–$1.7°$ is shown in Fig. 6, as well as the tensor-analysing power A_{zz}, extracted for excitation-energy bins of 100 keV. The structures prominent in Fig. 2 can also be localised in the A_{zz} spectrum around $E_x = 4.4$, 7.7, 9.3 and 10 MeV, but the analysing powers indicate some additional structure.

In the excitation-energy range, overlapping with the range discussed in the preceding section, the structure between $E_x =$ 4–5 MeV exhibits a negative A_{zz}, in agreement with the results from the fitting procedure. In addition, some substructure becomes obvious, which gets prominent by rearranging the data into 50 keV bins and zooming into the excitation-energy region 3.5–5.5 MeV, as can be seen in Fig. 7. One can recog-

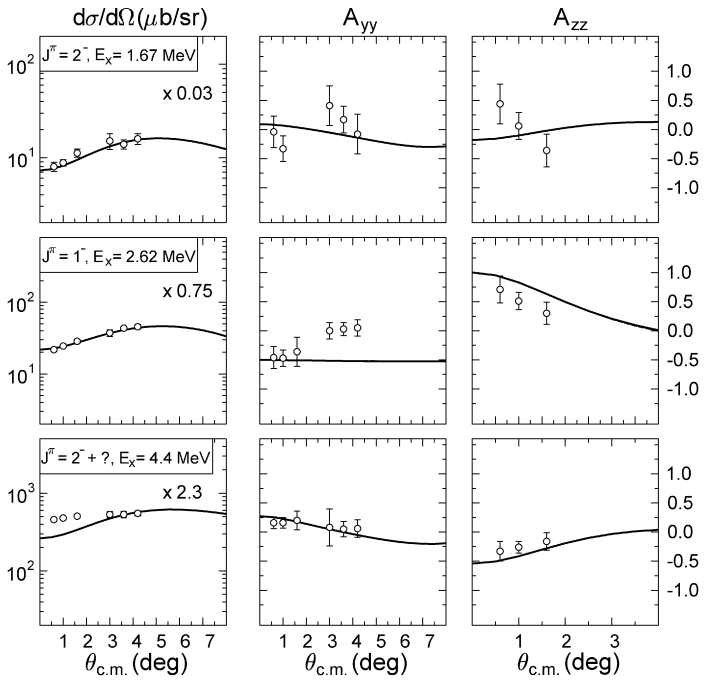

Fig. 5. Same as Fig. 4, but for negative-parity low-lying states. The A_{yy} point at $\theta_{\rm cm} = 1.6°$ for the first 2^- state is outside the boundaries of the graph. Its value is -2.11 ± 1.27.

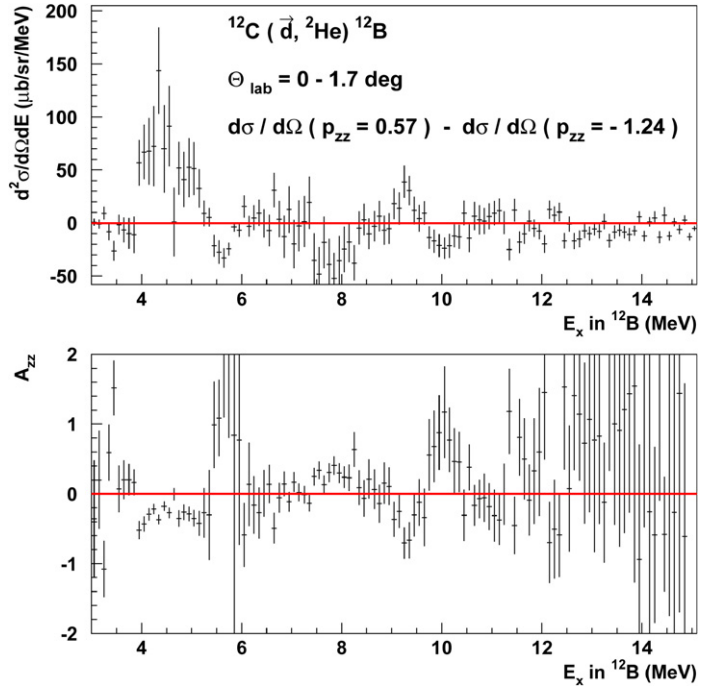

Fig. 6. Upper panel: difference between double-differential cross sections at $\theta_{\rm lab} = 0°$–$1.7°$ for the two beam polarisations as a function of excitation energy in ^{12}B. Lower panel: corresponding A_{zz} spectrum.

nise the bump at $E_x = 4.4$ MeV and a Gamow–Teller state at $E_x = 5$ MeV. Another state around $E_x = 4.0$ MeV with a large negative A_{zz} seems also to be present. The bump around $E_x = 4.4$ MeV seems to contain two states, which would be expected from Ref. [28]. Different shell-model calculations predict a $J^\pi = 0^-$ state around $E_x = 4$ MeV [18,19,32]. The theoretical predictions and the large negative A_{zz} suggest a $J^\pi = 0^-$ assignment for this state. The presence of such a state at this excitation energy would also explain the excess of cross section for small scattering angles that can be observed in Fig. 5.

At higher excitation energies, the large positive A_{zz} around $E_x = 5.5$ MeV is due to a $J^\pi = 3^+$ tabulated at $E_x = 5.612(8)$ MeV ($\Gamma = 140$ keV) [28]. The structure at $E_x = 7.5$ MeV also shows an, in average, positive A_{zz}, in disagreement with the results from Okamura et al. [10], where a small but negative A_{zz} was measured. A closer look at this structure

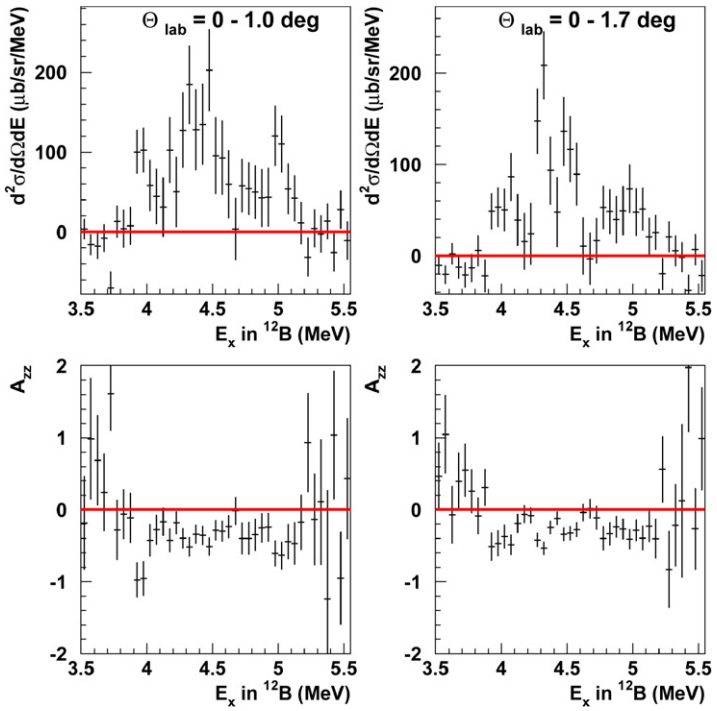

Fig. 7. Same as Fig. 6, but for two different angular bins and an excitation-energy range between 3.5 and 5.5 MeV. Left-hand side: $\theta_{\rm lab} = 0°$–$1°$. Right-hand side: $\theta_{\rm lab} = 0°$–$1.7°$.

Table 1
Differential cross sections and tensor-analysing powers of the ^{12}C($\vec{\rm d}$, ^{2}He) reaction at 171 MeV for well resolved states at low excitations energies for the most forward ^{2}He detection angle. The mixed state at 4.4 MeV depicted in Fig. 5 has not been taken into account

	θ (°)	$\frac{d\sigma}{d\Omega}$ ($\frac{\mu b}{sr}$)	A_{yy}	A_{zz}
$E_x = 0.00$ MeV, $J^\pi = 0^+$	0.6	1771.2 ± 14.3	0.04 ± 0.03	-0.01 ± 0.02
$E_x = 0.96$ MeV, $J^\pi = 2^+$	0.6	21.5 ± 1.5	-0.42 ± 0.23	0.93 ± 0.22
$E_x = 1.67$ MeV, $J^\pi = 2^-$	0.6	8.0 ± 0.9	-0.04 ± 0.27	0.44 ± 0.34
$E_x = 2.62$ MeV, $J^\pi = 1^-$	0.6	21.8 ± 1.4	-0.46 ± 0.19	0.71 ± 0.23
$E_x = 5.00$ MeV, $J^\pi = 1^+$	0.6	87.4 ± 3.4	0.28 ± 0.10	-0.53 ± 0.11

reveals that the low-energy part (from $E_x = 7.0$ to 7.5 MeV) has an almost vanishing A_{zz} and the high-energy part (from $E_x = 7.5$ to 8.0 MeV) definitely has a positive A_{zz}. Comparing to the A_{zz} obtained for the $J^\pi = 2^-$ state at $E_x = 4.4$ MeV and the $J^\pi = 1^-$ state at $E_x = 2.62$ MeV, it can be concluded that the high-energy part of the bump around $E_x = 7.5$ MeV consists of $J^\pi = 1^-$ strength, and that its low-energy part contains most probably $J^\pi = 2^-$ strength. This last conclusion is drawn from the angular distribution for A_{zz} of the ACCBA calculation presented in Fig. 5 for a $J^\pi = 2^-$ state. The same momentum transfer for an excited state around $E_x = 7$ MeV is obtained at a more forward angle than for an excited state at $E_x = 4.5$ MeV, meaning that the angular distribution for A_{zz} for a $J^\pi = 2^-$ state at higher excitation energy will be shifted to more forward scattering angles, thus yielding an A_{zz} closer to 0 for these angles.

Concerning the decomposition and the localisation of the J^π components of the IVSGDR the analysing powers yield the following result. Large negative analysing powers $A_{zz} \simeq -1$, the model-independent indication for the presence of the most elusive 0^- component, have been measured for the most forward angle spectra at $E_x = 4.0$ and 9.3 MeV in agreement with shell-model calculations [18,19,32]. The evidence for a concentration of 0^- strength at $E_x = 9.3$ MeV ($\Gamma = 330$ keV) further confirms the experimental results of Okamura et al. [10]. Evidence for the $J^\pi = 1^-$ component, which corresponds to a pure transverse transition, has been found in the high-energy part of the bump at $E_x = 7.5$ MeV. One state at $E_x = 7.85$ MeV seems to contain most of the strength. This is again in accordance with the shell-model calculation referred to above and in agreement with the conclusions of Inomata et al. regarding the mirror structure in ^{12}N [17]. A large concentration of positive A_{zz} is located at $E_x = 10.05(8)$ MeV, for which a width of $\Gamma = 470$ keV could be deduced from the data but no conclusive identification of the 1^- character could be achieved. The $J^\pi = 2^-$ component is localised in two energy regions, in the bump at $E_x = 4.5$ MeV and in the low-energy part of the bump at $E_x = 7.5$ MeV. Again, a good agreement with shell-model predictions is found.

In conclusion: For the ^{12}C(d, ^{2}He)^{12}B reaction, the coincident detection of decay neutrons at backward angles provides the selective means to remove the non-resonant con-

tinuum contributions in the cross section. The consistent description of the background by an empirical quasi-free approximation strongly indicates the dominant contribution of quasi-free scattering above excitation energy of 14 MeV. The consistent background determination allowed reliable extraction of tensor-analysing powers A_{xx} and A_{zz}. The unique energy resolution achievable at KVI allowed determination of analysing powers for well-resolved transitions up to 5 MeV excitation energy. The analysing powers of states with known spin and parity provided the means for the first-time for verification of model-independent predictions of analysing powers at extreme forward angles. In the continuum region, the analysing powers allowed identification of the J^π components of the IVSGDR, including a 0^- component located at $E_x = 9.3$ MeV. The results provide the stimulating basis to extend the analysing-power measurements to heavier nuclei and investigate the feasibility of the IVSGDR decomposition in complex nuclei, e.g., of relevance for $0\nu 2\beta$-decay measurements.

Acknowledgements

This work was performed as part of the research program of the *Stichting voor Fundamenteel Onderzoek der Materie* (*FOM*) with financial support from the *Nederlandse Organisatie voor Wetenschappelijk Onderzoek* (*NWO*).

References

[1] H.A. Bethe, et al., Nucl. Phys. A 324 (1979) 487.
[2] G.M. Fuller, W.A. Fowler, M.J. Newman, Astrophys. J. Suppl. Ser. 42 (1980) 447;
G.M. Fuller, W.A. Fowler, M.J. Newman, Astrophys. J. Suppl. Ser. 48 (1982) 279;
G.M. Fuller, W.A. Fowler, M.J. Newman, Astrophys. J. 252 (1982) 715;
G.M. Fuller, W.A. Fowler, M.J. Newman, Astrophys. J. 293 (1985) 1.
[3] W.G. Love, M.A. Franey, Phys. Rev. C 24 (1981) 1073.
[4] V.A. Rodin, et al., Phys. Rev. C 68 (2003) 044302.
[5] N. Auerbach, Phys. Rev. C 45 (1992) R514.
[6] S. Rakers, et al., Nucl. Instrum. Methods A 481 (2002) 253.
[7] C. Wilkin, D.V. Bugg, Phys. Lett. B 154 (1985) 243.
[8] C. Ellegaard, et al., Phys. Rev. Lett. 59 (1987) 974.
[9] H. Okamura, Phys. Lett. B 345 (1995) 1.
[10] H. Okamura, et al., Phys. Rev. C 66 (2002) 054602.
[11] G.G. Ohlsen, Rep. Prog. Phys. 35 (1972) 717.
[12] M.A. de Huu, PhD thesis, Rijksuniversiteit Groningen, 2004.
[13] H.R. Kremers, A.G. Drentje, in: R.J. Holt, M.A. Miller (Eds.), Polarized Gas Targets and Polarized Beams, in: AIP Conference Proceedings, vol. 421, AIP, New York, 1997, p. 507.
[14] A.M. van den Berg, Nucl. Instrum. Methods B 99 (1995) 637.
[15] H.J. Wörtche, Nucl. Phys. A 687 (2001) 321c.
[16] H. Laurent, et al., Nucl. Instrum. Methods A 326 (1992) 517.
[17] T. Inomata, et al., Phys. Rev. C 57 (1998) 3153.
[18] F.P. Brady, et al., Phys. Rev. C 43 (1991) 2284.
[19] N. Olsson, et al., Nucl. Phys. A 559 (1993) 368.
[20] X. Yang, et al., Phys. Rev. C 48 (1993) 1158.
[21] W.A. Sterrenburg, et al., Nucl. Phys. A 405 (1983) 109.
[22] C. Gaarde, et al., Nucl. Phys. A 422 (1984) 189.
[23] T. Ichihara, et al., Nucl. Phys. A 577 (1994) 93c.
[24] X. Yang, et al., Phys. Rev. C 52 (1995) 2535.
[25] B.D. Anderson, et al., Phys. Rev. C 54 (1996) 237.
[26] H. Sakai, et al., Nucl. Phys. A 599 (1996) 197c.
[27] A. Erell, et al., Phys. Rev. C 34 (1986) 1822.
[28] F. Ajzenberg-Selove, Nucl. Phys. A 506 (1990) 1.
[29] S. Strauch, F. Neumeyer, 1996, unpublished.
[30] H. Okamura, Phys. Rev. C 60 (1999) 064602.
[31] S. Rakers, et al., Phys. Rev. C 65 (2002) 044323, and references therein.
[32] T. Suzuki, H. Sagawa, Nucl. Phys. A 637 (1998) 547.